DOI 10.5012/bkcs.2010.31.5.1397

Refined Structure of Human NM23-H1 from a Hexagonal Crystal

Byeong-Gu Han,[†,§] Kyeongsik Min,[‡] Byung Il Lee,[†,*] and Sangho Lee[§,*]

[†]*Cancer Cell and Molecular Biology Branch, Division of Cancer Biology, Research Institute, National Cancer Center, Goyang, Gyeonggi 410-769, Korea. [*]E-mail: bilee@ncc.re.kr*
[‡]*Drug Discovery, Research & Development, LG Life Sciences, Daejeon 305-380, Korea*
[§]*Department of Biological Sciences, Sungkyunkwan University, Suwon 440-746, Korea. [*]E-mail: sangholee@skku.edu*
Received February 8, 2010, Accepted March 2, 2010

Key Words: NM23-H1, NDP kinase, Crystallization, Crystal structure

NM23-H1, also known as NDP kinase A (NDK-A), is the first identified metastasis suppressor gene.[1] It catalyzes the transfer of γ-phosphoryl group from a nucleoside triphosphate (NTP) donor onto a nucleoside diphosphate (NDP) acceptor through a transiently phosphorylated histidine residue. Other enzymatic activities of NM23-H1 include histidine kinase and 3'-5' exonuclease activity.[2] NM23-H1 shows high sequence identity to hexameric NM23-H2 (NDK-B), another member of NDK family.[3]

Multiple proteins including CKI, Aurora-A, Tiam1, Dbl1, KSR, ST-RAP and h-Prune have been reported to bind NM23-H.[4] H-Prune, which interacts and co-localizes with NM23-H1 in cytoplasm, plays a role in tumor progression and may function as a negative regulator of NM23-H1.[5,6] Crystal structures of wild type and mutant (H118G/F60W, S120G) NM23-H1 in complex with or without ADP have been reported. But no structural information of h-Prune is available yet.[7-9] We attempted to crystallize the h-Prune:NM23-H1 complex but only NM23-H1 was crystallized. Our crystals of NM23-H1 belong to the space group different from those of the previously reported structures of NM23-H1. We have determined the structure of the apo form of NM23-H1 from a hexagonal crystal at 2.1 Å resolution by molecular replacement. The refined model contains all 152 residues of NM23-H1 with good refinement statistics.

Crystallization of NM23-H1. Recombinant NM23-H1 and h-Prune were separately expressed in *Escherichia coli* and co-purified once the cell pellets were mixed and lysed together. However, we failed to observe the complex formation between the two proteins by size exclusion chromatography (data not shown). The two proteins were eluted at similar retention volumes because hexameric NM23-H1 and dimeric h-Prune happen to have similar total oligomeric molecular weights despite the differences in their monomeric molecular weights. The purified NM23-H1 and h-Prune mixture was subjected to crystallization screening. Needle shaped crystals were obtained using a reservoir solution consisting of 10% PEG 8000, 0.1 M Na/K phosphate pH 6.2, and 0.2 M NaCl. Crystals grew to approximate dimensions of 0.1 × 0.1 × 1 mm within three days (Crystal form 1). Form 1 crystals diffracted poorly and showed high diffraction anisotropy (Fig. 1). The best crystals were obtained by the addition of 10% (*v*/*v*) of 2 M sodium thiocyanate to the hanging drops (Crystal form 2). Form 2 crystals grew to approximate dimensions of 0.3 × 0.3 × 0.3 mm and diffracted to 2.1 Å with no diffraction anisotropy. The form 2 crystal belongs to the hexagonal space group $P6_122$ with unit cell parameters of $a = b = 154.4$, $c = 111.7$ Å. The presence of three subunits of NM23-H1 in the asymmetric unit gives a crystal volume per protein mass (V_M) of 3.33 Å^3 Da^{-1}, with a corresponding solvent content of 63.0%.[10] Data collection statistics are summarized in Table 1.

Structure of NM23-H1. The crystal structure of the apo NM23-H1 was determined at 2.1 Å resolution by molecular replacement. The model has been refined to R_{work} and R_{free} values of 22.4% and 24.2%, respectively. Refinement statistics are

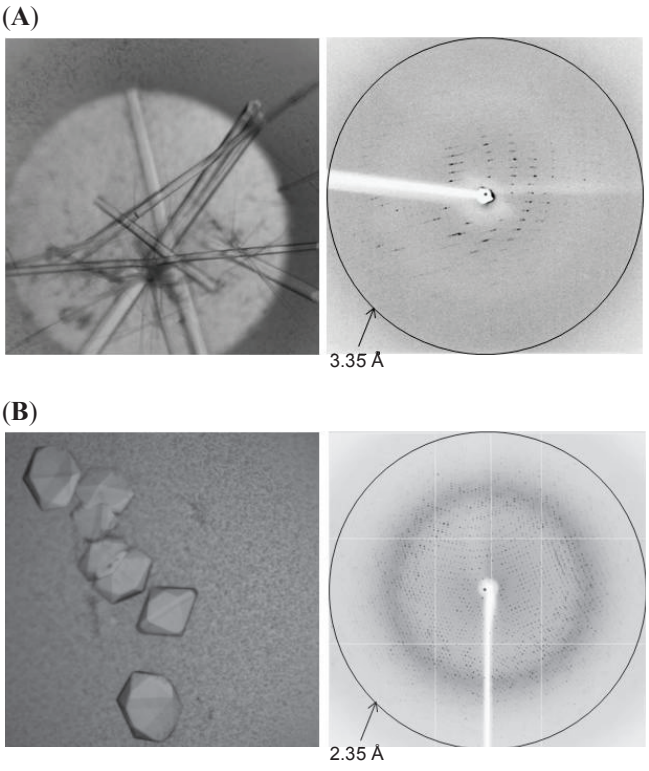

Figure 1. Crystals of NM23-H1. (**A**) Form 1 crystals of human NM23-H1. Their approximate dimensions are 0.1 × 0.1 × 1.0 mm and the best crystal diffracted to 4.0 Å with high diffraction anisotropy. (**B**) Form 2 crystals of human NM23-H1. Their approximate dimensions are 0.3 × 0.3 × 0.3 mm and the best crystal diffracted to 2.1 Å.

Table 1. Data collection and refinement statistics

Data Collection	
Beam Source	PF-5A
Space group	$P6_122$
Unit-cell parameters	
− Cell dimensions (Å)	$a = b = 154.4$, $c = 111.7$
− Angles (°)	$\alpha = \beta = 90$, $\gamma = 120$
Resolution range (Å)[a]	50-2.10 (2.15-2.10)
Total reflections/ Unique reflections	709,201/46,089
Completeness (%)	99.6 (98.6)
R_{merge} (%)[b]	10.1 (36.9)
Mean $I/\sigma(I)$	16.3 (4.3)
Refinement	
Resolution range for refinement (Å)	50-2.10
Number of protein atoms	3,634
Number of other molecules	
− Water/ Phosphate	292/2
Average *B*-factor (Å^2)	
− Protein atoms (A/B/C chain)	27.5/29.8/28.3
− Water/Phosphate	33.1/70.1
R.m.s. deviations from the ideal geometry	
− Bond length (Å)/ Bond angle(°)	0.006/0.897
R_{work}/R_{free}(%)[c]	22.4/24.2
Ramachandran plot[d]	94.9/4.4/0.8/0.0
PDB code	3L7U

[a]Values in parentheses are for the highest resolution shell. [b]$R_{merge} = \Sigma h \Sigma i \mid I(h,i) - \langle I(h) \rangle \mid / \Sigma h \Sigma i\, I(h,i)$, where $I(h,i)$ is the intensity of the i-th measurement of reflection h and $\langle I(h) \rangle$ is the mean value of $I(h, i)$ for all i measurements. [c]R_{free} is calculated for a randomly chosen 5% of reflections. [d]Percentage of non-glycine and non-proline residues in the most favored regions/additional allowed regions/generously allowed regions /disallowed regions.

summarized in Table 1. The refined monomer and hexamer models are shown in Fig. 2. There are three monomers of NM23-H1 in the asymmetric unit. The final model contains 458 residues for protein, two molecule of phosphate, and 292 water molecules in the asymmetric unit. Two extra residues (Ser-His) from N-terminal fusion tag were visible in the electron density map in chain B and all 152 amino acid residues in each subunit are clearly defined. The Ramachandran plot shows that 94.9% of non-glycine and non-proline residues are in the most favored regions, 4.4% of residues are in the additional allowed regions, 0.8% of residues in the generously allowed regions, and no residues in the disallowed regions.

Comparison of NM23-H1 structures reveals that our structure in $P6_122$ space group is similar to the known structures with subtle differences in atomic displacement factors. The r.m.s. differences between the model refined in the present study (chain A, PDB code 3L7U) and previously reported structures are 0.39 Å for 149 Cα atom pairs (Chain A of PDB code 1JXV; apo structure), and 0.97 Å for 151 Cα atom pairs (Chain A of PDB code 2HVD; ADP complex). The mean atomic displacement factors (*B*-factors) are significantly lower than previously reported models: average *B*-factor of our model is 29.0 Å^2 (27.5 Å^2 for chain A, 29.8 Å^2 for chain B, and 28.3 Å^2 for chain C) while those of apo structure (PDB code 1JXV) and ADP complex structure (PDB code 2HVD) are 45.0 Å^2 and 46.7 Å^2, respectively. *B*-factor plot for three comparable models is shown in Fig. 3.

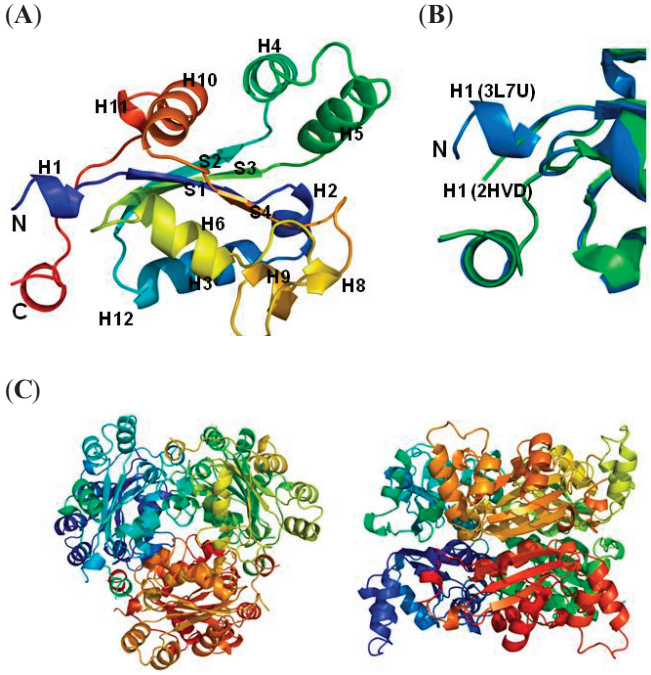

Figure 2. Overall structure of NM23-H1. **(A)** Ribbon diagram of NM23-H1 monomer (H: helix, S: strand). **(B)** Superposition of the N-terminal region (1-4) of NM23-H1 in the current structure (PDB code 3L7U in blue) and in the previously reported structure complexed with ADP (PDB code 2HVD in green). **(C)** Ribbon diagram of the homo-hexamer (Left for top view, Right for side view). Each monomer is colored differently.

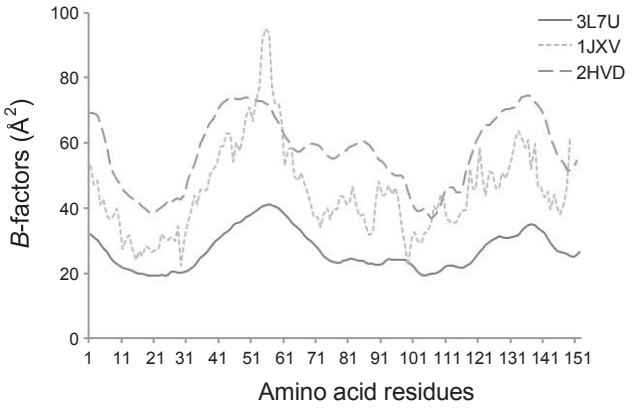

Figure 3. The *B*-factor plot for the apo structures (PDB code 3L7U in present study and PDB code 1JXV) and the ADP complex structure (PDB code 2HVD). For each structure, chain A was chosen for comparison. The *B*-factors averaged over all the atoms of each residue are shown.

The four N-terminal residues (1-4) of NM23-H1 in our model form a short H1 helix which was assigned as a random coil in a previously reported model complexed with ADP (Fig. 3). It has been reported that the K12Q mutant protein lacks all three enzymatic activities (3'-5' exonuclease, histidine kinase and nucleotide diphosphate kinase activities) of NM23-H1.[11] How-

ever, the E5A mutant shows a reduced 3'-5' exonuclease activity while it retains the other two enzymatic activities.[2,12] Glu-5 is located at the end of the H1 helix, implicating that the H1 helix may play a role in regulating the 3'-5' exonuclease activity of NM23-H1. The asymmetric unit contains three monomers of NM23-H1, exhibiting dihedral three-fold symmetry (D_3) and forming a trimer. A recent study suggests that the recombinant NM23-H1 usually exists as both hexamers and trimers. Therefore, the trimer in the asymmetric unit may represent the trimeric structure of NM23-H1.[13]

Materials and Methods

Protein expression and purification. NM23-H1 and h-Prune genes were amplified by polymerase chain reaction (PCR) and cloned into pET28b(+) (Novagen) using *Nde*I and *Xho*I restriction sites. This construction adds a 21-residue tag including hexa-histidine (MGSSHHHHHHSSGLVPRGSH and LEHH HHHH) to either the N-terminus of NM23-H1 or the C-terminus of h-Prune, for ease of protein purification. Two proteins were separately expressed in *E. coli* Rosetta2 (DE3) cells (Novagen). Cells transformed with the plasmids encoding either NM23-H1 or h-Prune were grown at 310 K in 2 L of Terrific Broth medium to an OD600 of 0.7, and induced by 0.01 or 0.1 mM isopropyl β-D-thiogalactopyranoside (IPTG) for NM23-H1 or h-Prune, respectively. The cells continued to grow at 291 K for 16 hours after IPTG induction and were harvested by centrifugation at 10,000 *g* for 10 min at 277 K. The cell pellet of NM23-H1 and h-Prune were then mixed, suspended in an ice-cold lysis buffer (25 mM Tris-HCl pH 7.4, 138 mM NaCl, 2 mM KCl, 10% (v/v) glycerol, 1 mM phenylmethylsulfonyl fluoride and 0.8 μM lysozyme) and homogenized by sonication. The crude lysate was subjected to centrifugation at 39,000 *g* for 60 min at 277 K, after which the cell debris was discarded. The first purification step utilized the hexa-histidine tag by means of a Ni^{2+}-NTA column (Qiagen). The eluents were pooled, concentrated and loaded to a HiLoad 16/60 Superdex-200 prep-grade column (GE Healthcare), which was pre-equilibrated with a buffer containing 50 mM phosphate buffer pH 6.6, 100 mM NaCl, 2 mM DTT, 1 mM EDTA. The purified protein was concentrated to 19 mg mL^{-1} using an YM10 membrane (Millipore).

Crystallization and structure determination. The initial crystallization conditions were searched by the sitting-drop crystallization method using 96-well plates (Axygen biosciences) at 296 K. The crystallization conditions containing 10% PEG 8000, 0.1 M Na/K phosphate pH 6.2, 0.2 M NaCl were further optimized by additive screen solutions. Each hanging drop was prepared by mixing 2 μL of the reservoir solution, 0.4 μL of 2.0 M sodium thiocyanate, and 2 μL of the protein solution. The crystal diffracted to 2.1 Å. The collected data were processed and scaled with *MOSFLM* and *SCALA*.[14,15] Data collection and processing statistics are shown in Table 1. The molecular replacement solution was found with *PHASER*[16] using a monomer of NM23-H1 as a search model (PDB code 1UCN). Iterative model building was performed using *COOT* and the model was refined with *REFMAC*.[17,18] All structural figures were generated using *PyMOL* (http://www.pymol.org/).

Protein Data Bank Accession code. Structure factors and atomic coordinates have been deposited in Protein Data Bank with an access code of 3L7U.

Acknowledgments. We thank beamline staffs for assistance during data collection at beamline BL-5A of Photon Factory, Japan. This work was supported by National Research Foundation of Korea Grants funded by the Korean Government (KRF-2007-521-C00240 and KRF-2008-314-C00224) to S. Lee.

References

1. Ouatas, T.; Abdallah, B.; Gasmi, L.; Bourdais, J.; Postel, E.; Mazabraud, A. *Gene* **1997**, *194*, 215.
2. Kaetzel, D. M.; McCorkle, J. R.; Novak, M.; Yang, M.; Jarrett, S. G. *Mol. Cell. Biochem.* **2009**, *329*, 161.
3. de la Rosa, A.; Williams, R. L.; Steeg, P. S. *Bioessays* **1995**, *17*, 53.
4. Kim, H. D.; Youn, B.; Kim, T. S.; Kim, S. H.; Shin, H. S.; Kim, J. *Mol. Cell Biochem.* **2009**, *329*, 167.
5. Reymond, A.; Volorio, S.; Merla, G.; Al-Maghtheh, M.; Zuffardi, O.; Bulfone, A.; Ballabio, A.; Zollo, M. *Oncogene* **1999**, *18*, 7244.
6. Galasso, A.; Zollo, M. *Mol. Cell Biochem.* **2009**, *329*, 149.
7. Min, K.; Song, H. K.; Chang, C.; Kim, S. Y.; Lee, K. J.; Suh, S. W. *Proteins* **2002**, *46*, 340.
8. Chen, Y.; Gallois-Montbrun, S.; Schneider, B.; Veron, M.; Morera, S.; Deville-Bonne, D.; Janin, J. *J. Mol. Biol.* **2003**, *332*, 915.
9. Giraud, M. F.; Georgescauld, F.; Lascu, I.; Dautant, A. *J. Bioenerg. Biomembr.* **2006**, *38*, 261.
10. Matthews, B. W. *J. Mol. Biol.* **1968**, *33*, 491.
11. Ma, D.; McCorkle, J. R.; Kaetzel, D. M. *J. Biol. Chem.* **2004**, *279*, 18073.
12. Yoon, J. H.; Singh, P.; Lee, D. H.; Qiu, J.; Cai, S.; O'Connor, T. R.; Chen, Y.; Shen, B.; Pfeifer, G. P. *Biochemistry* **2005**, *44*, 15774.
13. Garzia, L.; D'Angelo, A.; Amoresano, A.; Knauer, S. K.; Cirulli, C.; Campanella, C.; Stauber, R. H.; Steegborn, C.; Iolascon, A.; Zollo, M. *Oncogene* **2008**, *27*, 1853.
14. Leslie, A. G. *Acta Crystallogr. D Biol. Crystallogr.* **2006**, *62*, 48.
15. Kabsch, W. *J. Appl. Crystallogr.* **1988**, *21*, 916.
16. McCoy, A. J.; Grosse-Kunstleve, R. W.; Adams, P. D.; Winn, M. D.; Storoni, L. C.; Read, R. J. *J. Appl. Crystallogr.* **2007**, *40*, 658.
17. Emsley, P.; Cowtan, K. *Acta Crystallogr. D Biol. Crystallogr.* **2004**, *60*, 2126.
18. Murshudov, G. N.; Vagin, A. A.; Dodson, E. J. *Acta Crystallogr. D Biol. Crystallogr.* **1997**, *53*, 240.